



Published in final edited form as:

*J Neurosci Methods*. 2008 June 30; 171(2): 218–225. doi:10.1016/j.jneumeth.2008.03.007.

## Characterizing molecular probes for diffusion measurements in the brain

Gurjinder Kaur<sup>1</sup>, Sabina Hrabetova<sup>2,3</sup>, David N. Guilfoyle<sup>1</sup>, Charles Nicholson<sup>3</sup>, and Jan Hrabe<sup>1,2,\*</sup>

<sup>1</sup>Center for Advanced Brain Imaging, Nathan S. Kline Institute for Psychiatric Research, Orangeburg, New York

<sup>2</sup>Department of Anatomy and Cell Biology, SUNY Downstate Medical Center, Brooklyn, New York

<sup>3</sup>Department of Physiology and Neuroscience, NYU School of Medicine, New York, New York

### Abstract

Brain diffusion properties are at present most commonly evaluated by magnetic resonance (MR) diffusion imaging. MR cannot easily distinguish between the extracellular and intracellular signal components, but the older technique of Real-Time Iontophoresis (RTI) detects exclusively extracellular diffusion. Interpretation of the MR results would therefore benefit from auxiliary RTI measurements. This requires a molecular probe detectable by both techniques. Our aim was to specify a minimum set of requirements that such a diffusion probe should fulfill and apply it to two candidate probes: the cation tetramethylammonium (TMA<sup>+</sup>), used routinely in the RTI experiments, and the anion hexafluoroantimonate (SbF<sub>6</sub><sup>-</sup>). Desirable characteristics of a molecular diffusion probe include predictable diffusion properties, stability, minimum interaction with cellular physiology, very slow penetration into the cells, and sufficiently strong and selective MR and RTI signals. These properties were evaluated using preparations of rat neocortical slices under normal and ischemic conditions, as well as solutions and agarose gel. While both molecules can be detected by MR and RTI, neither proved an ideal candidate. TMA<sup>+</sup> was very stable but it penetrated into the cells and accumulated there within tens of minutes. SbF<sub>6</sub><sup>-</sup> did not enter the cells as readily but it was not stable, particularly in ischemic tissue and at higher temperatures. Its presence also resulted in a decreased extracellular volume. These probe properties help to interpret previously published MR data on TMA<sup>+</sup> diffusion and might play a role in other diffusion experiments obtained with them.

### Keywords

Extracellular space; Intracellular space; Ion-selective microelectrodes; Real-time iontophoretic method; MR diffusion spectroscopy; Tetramethylammonium (TMA<sup>+</sup>); Hexafluoroantimonate (SbF<sub>6</sub><sup>-</sup>)

---

\*Corresponding author: Jan Hrabe, Center for Advanced Brain Imaging, Nathan S. Kline Institute for Psychiatric Research, 140 Old Orangeburg Road, Orangeburg, NY 10962, USA, Email: hrabe@nki.rfmh.org, Phone: 1-845-398-5471, Fax: 1-845-398-5472.

**Publisher's Disclaimer:** This is a PDF file of an unedited manuscript that has been accepted for publication. As a service to our customers we are providing this early version of the manuscript. The manuscript will undergo copyediting, typesetting, and review of the resulting proof before it is published in its final citable form. Please note that during the production process errors may be discovered which could affect the content, and all legal disclaimers that apply to the journal pertain.

## Introduction

Diffusion is the most important transport mechanism in the brain, both inside neurons and glial cells, and in the extracellular space (ECS) surrounding them. Diffusion in the ECS has been extensively studied and significant changes of diffusion parameters were found in the course of normal development (Lehmenkühler et al., 1993; Vorisek and Sykova, 1997) and aging (Sykova et al., 1998; Sykova et al., 2002) as well as in response to many pathological processes such as ischemia and stroke (Rice and Nicholson, 1991; Sykova et al., 1994; Hrabetova et al., 2002), osmotic stress (Krizaj et al., 1996; Kume-Kick et al., 2002), epilepsy (Schwindt et al., 1997; Slais et al., 2008), and spreading depression (Mazel et al., 2002). Much less is known about intracellular diffusion but measurements in ischemia and excitotoxic injury documented reductions in metabolite diffusion coefficients (Wick et al., 1995). The diffusion process can serve also as a useful tool for indirect exploration of the geometrically complex brain environment (Nicholson, 2001; Kume-Kick et al., 2002; Hrabetova et al., 2003; Hrabe et al., 2004).

Among several methods for measuring diffusion in brain tissue, Magnetic Resonance (MR) is currently the most popular choice, particularly in its Diffusion Tensor Imaging (DTI) variant (Basser et al., 1994), which has already been deployed in clinical settings. The MR method typically employs water as the diffusion probe molecule and quantifies its apparent diffusion coefficient (ADC). Unfortunately, water is found in both intracellular and extracellular brain compartments, and it also crosses cellular membranes on a time scale comparable to typical diffusion times, making separation of the signals from these compartments particularly difficult (Quirk et al., 2003). Consequently, a change in ADC cannot reliably be attributed exclusively to the extracellular or intracellular compartment, to a combination of the two, or to a change in the cellular membrane permeability for water.

The older Real-Time Iontophoretic (RTI) method (Nicholson and Phillips, 1981) uses small ions as the diffusion probe molecules. Ion-selective microelectrodes (ISMs) detect the diffusing ions released by iontophoresis from a micropipette about a hundred micrometers away. If the probe does not penetrate the cell membranes or otherwise leave the ECS in the course of an RTI experiment (on the order of minutes), or if the loss of the probe from the ECS is taken into account, the method can obtain the ECS diffusion coefficient with no intracellular component present. Exclusive sensitivity of RTI to ECS diffusion makes it a potentially valuable aid in interpretation of the MR measurements. With a suitable diffusion probe molecule employed under similar conditions by both the MR and the RTI methods, the MR signal could be more reliably interpreted. Moreover, if the rate of probe penetration into the cells was quantitatively established, separation of the intracellular MR signal would become feasible as long as the rate was sufficiently slow (on the order of hours).

One probe frequently used in RTI, tetramethylammonium ( $\text{TMA}^+$ ), was employed in MR diffusion experiments by Kroenke and colleagues (Kroenke et al., 2003). While they successfully detected diffusion of  $\text{TMA}^+$  in a rat brain *in vivo*, they encountered difficulties matching their results to those obtained by the RTI method. Their analysis hinted at the possibility that the  $\text{TMA}^+$  probe may have entered the brain cells too rapidly to allow the detection of an exclusively extracellular signal.

An ideal molecular diffusion probe should have several key features: predictable diffusion properties, chemical stability in artificial media and in the brain, and negligible interaction with cell physiology. The rate of probe penetration into the cells has to be known and it must be sufficiently slow to accommodate the time scale of RTI experiments. The RTI and MR signals have to be sufficiently strong and selective. A subset of these characteristics have been obtained in the past for several probes used in the RTI studies (Nicholson and Phillips, 1981; Rice and

Nicholson, 1991; Nicholson, 1992). However, these criteria have never been systematically explored for the probe ions used in past and present work. Such an examination becomes critical when MR and RTI measurements are combined but the results are also relevant for either of these methods used alone.

Based on a list of probes employed in RTI experiments (Nicholson and Phillips, 1981; Nicholson, 1993), we have selected the two that also provided a reliable MR signal: TMA<sup>+</sup> and SbF<sub>6</sub><sup>-</sup> (hexafluoroantimonate anion). A potential benefit of SbF<sub>6</sub><sup>-</sup> is the ease with which fluorine MR signal can be detected, without the difficulties associated with water signal suppression necessary for detection of TMA<sup>+</sup>.

## Materials and Methods

Several model diffusion environments were used: normal rat brain slices (400 μm), ischemic rat brain slices (1000 μm), solutions, and agarose gel. ISMs were used to determine the absolute values of probe ion concentrations. These were required for evaluation of the probe diffusion properties and its stability, and were equally important in the RTI and in the homogenization experiments. The RTI experiments served to extract the free diffusion coefficients of the probe in dilute agar gel, as well as the ECS volume fractions in brain tissue. The homogenization experiments provided estimates of the intracellular probe concentration and established the time course of its penetration into the cells. Finally, an MR spectroscopic study of the SbF<sub>6</sub><sup>-</sup> at 7 Tesla obtained independent information on this probe behavior.

### Rat brain slices and agarose gels

All animal experiments were conducted at NYU School of Medicine in accordance with NIH guidelines and local IACUC regulations. Adult Sprague-Dawley female rats (150–250 g) were anesthetized with sodium pentobarbital (50 mg kg<sup>-1</sup> IP) and decapitated with a guillotine. The brains were extracted from the skulls and dipped in ice-cold artificial cerebrospinal fluid (ACSF).

Brain slices were prepared as described previously (Hrabetova et al., 2002). Coronal brain slices 1000 μm or 400 μm thick were cut on a vibrating-blade microtome (VT 1000 S; Leica Instrument GmbH, Nussloch, Germany). Slices were immediately transferred and incubated in ACSF at room temperature or at 34°C. The composition of the ACSF, in mM, was: NaCl 124, KCl 5, NaHCO<sub>3</sub> 26, NaH<sub>2</sub>PO<sub>4</sub> 1.25, D-glucose 10, MgCl<sub>2</sub> 1.3, and CaCl<sub>2</sub> 1.5. The ACSF was continually gassed with a mixture of 95% O<sub>2</sub> and 5% CO<sub>2</sub> to buffer the pH at 7.4. Osmolality of the ACSF (300 ± 5 mOsm kg<sup>-1</sup>) was measured with a freezing point-depression osmometer (Osmette A #5002; Precision Systems Inc., Natick, MA, USA).

Agarose gel, representing an obstacle-free diffusion medium, was prepared as a 0.3% mixture of agarose (NuSeive, FMC BioProducts, Rockland, ME, USA) in 150 mM solution of NaCl containing 0.5 mM of TMA<sup>+</sup>.

### Ion-selective and iontophoretic microelectrodes

A previously established method (Nicholson, 1993) using double-barreled theta glass (Warner Instrument Corp., Hamden, CT, USA) was followed to manufacture the ISMs sensitive to TMA<sup>+</sup> (*MW* 74) or SbF<sub>6</sub><sup>-</sup> (*MW* 236). For TMA<sup>+</sup> ISM, the tip of an ion detecting barrel contained an exchanger based on tetraphenylborate (Corning exchanger 477317, currently available as IE 190 from WPI, Sarasota, FL, USA). The barrel was backfilled with 150 mM solution of TMA<sup>+</sup> chloride. A more detailed account of the composition and selectivity characteristics of the ion exchanger are to be found in the paper by Ammann and Simon (1987). For SbF<sub>6</sub><sup>-</sup> ISM, the ion detecting tip contained 10 mM Crystal Violet dye exchanger

(J.T. Baker Chemicals, Phillipsburg, NJ, USA) dissolved in 3-nitro-*O*-xylene (Fisher Scientific, Pittsburgh, PA, USA), and the barrel was backfilled with 150 mM solution of NaSbF<sub>6</sub>. Additional information about the anion exchanger is given by Phillips and Nicholson (1981). The reference barrels of both ISMs were filled with 150 mM solution of NaCl.

Each ISM was calibrated in a series of solutions with geometrically increasing concentrations of the ion of interest (e.g., 0.125, 0.25, 0.5, 1, and 2 mM) added to 150 mM background concentration of NaCl. The calibration data were fitted to the Nikolsky equation to obtain the slope and interference parameters of the microelectrode (Nicholson, 1993). Stability of calibrating solutions was verified separately by comparing the ISM voltages of aged solutions with those freshly prepared.

The iontophoretic microelectrodes were pulled from the same type of double-barreled theta glass. However, both barrels were filled with 150 mM solution of TMA<sup>+</sup> chloride or NaSbF<sub>6</sub>.

### Probe stability

The stability of the TMA<sup>+</sup> and SbF<sub>6</sub><sup>-</sup> in a physiological solution of ACSF was evaluated by recording the probe concentration as a function of time, both at room temperature and at 34° C. The concentration was determined with a previously calibrated ISM. The raw electrode voltages were converted to ionic concentrations using Nikolsky equation (Nicholson, 1993). The probe solutions in ACSF were prepared fresh prior to starting the experiments and kept in beakers constantly gassed with a mixture of 95% O<sub>2</sub> and 5% CO<sub>2</sub> to buffer the pH at 7.4. Temperature was maintained within 1°C of the desired value with a hot plate and a thermometer.

It was important to verify that probe concentration did not depend on the presence of brain tissue. To this end, we used the two slice preparations (normal and ischemic) described above. The slices were transferred into a slice chamber system (Model BSC-BU with BSC-ZT attachment; Warner Instruments, Hamden, CT, USA) and bathed in ACSF gassed with a mixture of 95% O<sub>2</sub> and 5% CO<sub>2</sub> containing 5 mM of SbF<sub>6</sub><sup>-</sup> or 4 mM of TMA<sup>+</sup>. An inflow rate of 2.5 mL min<sup>-1</sup> was maintained by a peristaltic pump (Gilson Minipulse 3, Gilson, Inc., Middleton, WI, USA). Solution outflow was driven by vacuum, thus maintaining a constant bath level in the chamber (Fig. 1). Normal slices were exposed to the probe solution for at least 1 hour and thick slices for at least 2 hours prior to measurement to achieve a uniform penetration (Nicholson and Hounsgaard, 1983). A calibrated ISM was then held vertically over the slice in a manually controlled micromanipulator, and the tip was gradually lowered into the cortex region of the brain slice to obtain a vertical profile of concentration across the slice. In the thin slice, concentrations were recorded at depths 0 and 200 μm (slice center). In the thick slice, they were recorded every 100 μm from 0 to 1000 μm.

### RTI diffusion measurements

It is well documented that low concentrations of TMA<sup>+</sup> do not noticeably affect the brain slice physiology, at least not on a time scale of the RTI measurements (Nicholson and Phillips, 1981; Rice and Nicholson, 1991; Kume-Kick et al., 2002). However, the SbF<sub>6</sub><sup>-</sup> probe has not been tested in this respect. Because the ECS volume fraction is a sensitive indicator of brain slice viability (Rice and Nicholson, 1991), we employed RTI diffusion measurements (using the TMA<sup>+</sup> probe) to assess the effect of SbF<sub>6</sub><sup>-</sup> presence in the bathing solution on the slice well-being. A similar approach was used previously for other background molecules (Hrabetova and Nicholson, 2000).

Microelectrode arrays for RTI measurements were prepared following an established procedure (Nicholson, 1993). An iontophoretic microelectrode was glued with dental cement to the ISM. Prior to gluing, the tapered end of the iontophoretic electrode was bent at an angle, making the final few millimeters of both microelectrodes parallel to each other. The tip separation, measured under a microscope, was typically 100–150  $\mu\text{m}$ .

Diffusion measurements were performed in the brain slice chamber (Fig. 1). However, the ACSF bath solution now contained 0.5 mM of  $\text{TMA}^+$  and 10 mM of  $\text{SbF}_6^-$ . The microelectrode array was lowered into a separate agar well (for auxiliary measurements of the transport number of the iontophoretic source) or to the center of brain slice. A constant forward bias current of 20 nA was delivered from a custom high-impedance unit to the iontophoretic microelectrode to stabilize its transport number (Nicholson, 1993). The time-dependent diffusion source took the form of an additional current pulse of 40 to 100 nA, lasting typically 50 s. The ISM positioned nearby served as a detector. The DC potential recorded from its reference barrel was continuously subtracted from the ion-selective barrel in a dual-channel preamplifier (model IX2–700, Dagan Corp., Minneapolis, MN, USA). Both signals (DC and subtraction) were low-pass filtered at 6 Hz and further amplified by a CyberAmp 320 (Axon-CNS, Molecular Devices, Sunnyvale, CA), monitored on a chart recorder, and digitized and stored on a PC-compatible computer.

An appropriate solution to the diffusion equation (Nicholson, 2001; Hrabetova and Nicholson, 2007) was fitted to the data using a custom Matlab (MathWorks, Natick, MA, USA) program to extract iontophoretic source transport number and distance between the microelectrode tips (from the agar measurements combined with the known value of  $D$  for  $\text{TMA}^+$ ), or ECS volume fraction  $\alpha$  (from the brain slice measurements). The ECS volume fraction is simply the percentage of the brain tissue occupied by the ECS.

### Probe penetration into the cells

Probe penetration into the cells was assessed by a brain homogenization experiment. Its basic idea is simple: brain slices are incubated for a period of time in the probe solution. The probe concentrations in the bath and in the ECS are readily accessible to an ISM but the intracellular concentration cannot be directly detected. However, when the brain slices are homogenized in a small amount of bath solution, most cellular membranes are disrupted and the intracellular and extracellular compartments merge with the bath. Probe concentration in the homogenate can be measured by an ISM and used to calculate the original intracellular probe concentration, providing we know the volumes of the individual compartments at the time of their destruction.

To arrive to an appropriate formula for intracellular concentration, we start by counting the probe molecules in all compartments: let  $n_i$ ,  $n_e$ ,  $n_d$ , and  $n_b$  be in turn the molecular counts inside the cells, in the ECS, in the dry matter, and in the bath. The total number of probe molecules, unaffected by homogenization, is then

$$n_T = n_i + n_e + n_d + n_b \quad (1)$$

Probe molecular count  $n$  in any compartment can be expressed via its molar concentration  $c$  and compartmental mass  $m$  as  $n = (N_A / \rho) c m$ , where  $N_A$  is Avogadro's number and  $\rho$  is the mass density ( $\rho = m / V$ , where  $V$  is the compartmental volume). If we assume that the density is almost identical in all compartments (Krizaj et al., 1996), the term  $N_A / \rho$  will be identical for all compartments and can be safely discarded. From Eq. (1), we then obtain intracellular concentration

$$c_i = \frac{c_T m_T - c_e m_e - c_b m_b}{m_i} \quad (2)$$

where we also assumed that no probe has accumulated in the dry matter compartment. All the concentrations on the right side of Eq. (2) can be measured by ISMs, and the masses  $m_T$  and  $m_b$  are easily obtained by accurate weighing. Their difference  $m_s = m_T - m_b$  is the mass of the slices without any bath solution. If densities in all compartments are identical,  $m_e$  can be calculated from a known ECS volume fraction  $\alpha = V_e / V_s = m_e / m_s$  and a total mass  $m_T = m_i + m_e + m_d + m_b = m_s + m_b$ :

$$m_e = \alpha(m_T - m_b) = \alpha m_s \quad . \quad (3)$$

For  $m_i$  we similarly have  $m_i = m_T - m_e - m_d - m_b = (1 - \alpha) m_s - m_d$ . The dry weight  $m_d$  can be taken from previously published results in normal and ischemic brain slices (Hrabetova et al., 2002). It is commonly reported in the form of dry weight ratio  $\beta = m_d / m_s$ . The mass of the intracellular compartment can then be expressed as

$$m_i = (1 - \alpha)m_s - \beta m_s = (1 - \alpha - \beta)m_s \quad . \quad (4)$$

Substituting from Eq. (3) and Eq. (4) into Eq. (2), we finally obtain a useful formula for extracting the intracellular probe concentration:

$$c_i = \frac{c_T m_T - \alpha c_e m_s - c_b m_b}{(1 - \alpha - \beta)m_s} \quad . \quad (5)$$

The homogenization procedure was used to determine the rates of  $\text{TMA}^+$  and  $\text{SbF}_6^-$  cellular penetration in the following manner: Normal and ischemic cortical slices were incubated in a bath of ACSF containing 0.5 mM of  $\text{TMA}^+$  or 10 mM of  $\text{SbF}_6^-$  at room temperature or at 34°C. After a predetermined incubation period, the slices were collected from the bath and the excess surface moisture was carefully removed. They were placed in an Eppendorf centrifuge tube together with a known amount of their bath solution (800  $\mu\text{L}$ ). The tube was weighed twice, once before and once after adding the slices. The slices were then ultrasonically homogenized (Sonic Dismembrator-60, Fisher Scientific, Pittsburgh, PA, USA) to break the cellular membranes. The ion concentration in the homogenate was measured with a calibrated ISM. The bath concentration was obtained with the same ISM immediately before homogenization.

This procedure was performed following several different incubation periods. For  $\text{TMA}^+$ , the incubation periods were 0, 0.5, 1, 2, 4, and 6 hours, while the sample slices incubated in  $\text{SbF}_6^-$  were taken at 0, 2, 3, 4, 5, and 6 hours. ECS volume fractions for  $\text{TMA}^+$  in normal and thick slices were taken from a previous study (Hrabetova et al., 2002). The RTI experiments described earlier provided the corresponding volume fractions in the presence of  $\text{SbF}_6^-$ .

### Magnetic resonance spectroscopy

As will be shown in the Results, ISM measurements of the  $\text{SbF}_6^-$  stability indicated degradation of this probe with time. We employed fluorine MR spectroscopy to independently verify this finding and gain more insight into the degradation process.

All MR data were acquired on a 7.0 T spectrometer (Magnetic Resonance Research Systems, formerly SMIS, Guildford, UK) attached to a 40 cm bore magnet (Magnex Scientific, Yarnton, UK). The system was equipped with a 10 cm internal diameter gradient coil insert (Magnex Scientific, Yarnton, UK) and a 16 mm diameter transmit-receive surface coil tunable to  $^{19}\text{F}$  and  $^1\text{H}$  frequencies (Doty Scientific, Inc., Columbia, SC, USA).

A 10 mM  $\text{SbF}_6^-$  solution in ACSF was freshly prepared and gassed as described earlier. It was supplied at a flow rate of 2.5 mL  $\text{min}^{-1}$  by peristaltic pump (Gilson Minipulse 3, Gilson, Inc., Middleton, WI, USA) to a sealed nonmagnetic chamber (model RC-21B, Warner Instruments, Hamden, CT, USA), placed horizontally in a fabricated acrylic holder at the magnet isocenter. The flow was briefly stopped during data acquisition to prevent flow artifacts. For calibration



and verification purposes, the  $\text{SbF}_6^-$  measurements were preceded and followed by acquiring a spectrum of sodium trifluoroacetate (10 mM), a compound commonly employed in this capacity. For comparison, we also acquired spectral peaks of NaF (5 mM) and HF (10 mM).

The system was first carefully shimmed to compensate for magnetic field inhomogeneities. A complete acquisition sequence at each time point consisted of a rectangular radiofrequency pulse (duration 100  $\mu\text{s}$ , flip angle 90 degrees) followed by a free induction decay (FID), repeated 100 times every 5 s. The averaged FID signal was Fourier-transformed and phase-corrected to obtain the spectrum. This procedure was repeated at several time points from 0 to 120 min. The peak amplitude of the  $\text{SbF}_6^-$  resonance was measured in arbitrary units at time  $t = 0$  and assumed to reflect a 100% concentration. All subsequent amplitude measurements were normalized to this level, giving the relative change in concentration over time.

## Results

### Chemical stability

The probe molecule should remain stable in the solutions serving the ISM calibration procedure, in the ACSF solution, and in the brain tissue under all expected experimental conditions. If it is not entirely stable, at least its degradation rate has to be stable and known.

We first tested stability of  $\text{TMA}^+$  and  $\text{SbF}_6^-$  in the calibrating solutions of a probe in 150 mM NaCl, by comparing ISM signals from older solutions with those obtained from a freshly made stock (data not shown). The  $\text{TMA}^+$  signal was stable whereas the  $\text{SbF}_6^-$  exhibited a slight drop over 24 hours. A new set of  $\text{SbF}_6^-$  calibrating solutions was therefore prepared before every experiment.

Next, the probes were tested in solutions of ACSF over a period typical for diffusion experiments (Fig. 2). Concentrations of  $\text{TMA}^+$  did not demonstrate any significant change with time (Fig. 2a). In contrast,  $\text{SbF}_6^-$  was significantly degraded over time and the degradation rate was sensitive to temperature (Fig. 2b). In solutions 2–5 hours old, the degradation rate was approximately 3.9% per hour at room temperature, and reached more than 6% per hour at 34°C. We therefore performed most subsequent  $\text{SbF}_6^-$  experiments at room temperature.

To test stability in the brain tissue, depth profiles of probe concentrations were acquired in normal and ischemic slices preincubated in probe solutions at room temperature (Fig. 3). The incubation period was sufficiently long for a probe to penetrate the slice. A record obtained at the slice center over time confirmed that the initially rising concentration became constant during this period. A stable probe should exhibit an entirely flat profile thereafter. Such profiles were indeed recorded for the  $\text{TMA}^+$  probe in normal slices (data not shown) as well as in ischemic slices (Fig. 3).

The  $\text{SbF}_6^-$  depth profiles were very different. In the normal slice, probe concentration at the slice center (depth 200  $\mu\text{m}$ ) decreased by 4.5% with respect to its surface value (data not shown). A much more profound drop of 58.6% was found in the center of an ischemic slice (depth 500  $\mu\text{m}$ , Fig. 3). Concentrations recovered at greater depths as the tip of the ISM approached the lower surface of the slice. The microelectrode was not allowed to enter the ACSF solution below the slice to prevent damaging it on the mesh supporting the slice.

### Effect on brain tissue

The concentration profiles described above suggest that the slice condition may be affected by the  $\text{SbF}_6^-$  probe, particularly in the ischemic slice. This was tested by measuring the ECS volume fractions using the  $\text{TMA}^+$  probe in the presence of 10 mM  $\text{SbF}_6^-$  added to the bath ACSF for a period of 4–5 hours. The results obtained from three or more slices in each group

show that  $\text{SbF}_6^-$  probe caused cellular swelling in both normal and ischemic slices. The ECS volume fraction in normal slices was reduced from the commonly reported 24% (e.g., Hrabetova et al., 2002) to a mere 11% (SD 1%). The ECS volume fraction of 15% in ischemic slices (Hrabetova et al., 2002) was reduced to a very similar value ( $\alpha = 10 \pm 1\%$ ). However, these slices contained cells that were already swollen due to oxygen deprivation. Thus, additional ECS shrinkage inflicted by the  $\text{SbF}_6^-$  probe appeared to be less pronounced. In several preparations, a phenomenon resembling spreading depression (Somjen, 2001) was observed shortly after  $\text{SbF}_6^-$  application, leading to cellular swelling reflected in a spontaneous increase in  $\text{TMA}^+$  concentration in the ECS with no apparent recovery afterwards.

In contrast to  $\text{SbF}_6^-$ , the  $\text{TMA}^+$  probe interference with brain tissue physiology had been carefully tested before (Nicholson and Phillips, 1981; Rice and Nicholson, 1991; Hrabetova et al., 2002) and no measurable decline in the tissue viability was observed.

### Penetration of probes into cells

We evaluated penetration of both diffusion probes into normal and ischemic cells at several time points extending up to 6 hours of incubation in the probe solutions (Fig. 4). The homogenization procedure described in the Methods was followed, using Eq. (5) to calculate the intracellular concentration at every time point.

Fig. 4 shows that the intracellular concentration of  $\text{TMA}^+$  increases during the first hours of incubation. Surprisingly, the cellular influx continues after the intracellular concentration exceeds the extracellular. The intracellular concentration reaches a plateau after about 3 hours, at a value of approximately 300% of the ECS concentration in normal slices, and half as high in ischemic slices. Note that the initial rate of influx is so fast that it coincides with the probe diffusion into the slice, that is, before the probe ECS concentration throughout the slice reaches the bath level. Fig. 4 therefore likely underestimates the early influx rates.

Interpretation of  $\text{SbF}_6^-$  data was complicated by its degradation, which we showed to be dependent on depth within the slice. The homogenization procedure also abruptly changed the chemical environment and induced a further sudden shift in concentration. This was apparent at time  $t = 0$  when both the extracellular and intracellular concentrations should be close to zero. Instead, the intracellular concentrations exhibited large negative offsets corresponding to about 30% probe loss due to homogenization. We can therefore interpret no more than the relative concentration changes with incubation time. In contrast to  $\text{TMA}^+$ , the  $\text{SbF}_6^-$  behaved similarly in normal and ischemic slices, and concentration increments were spread more evenly over the entire incubation period; there was no apparent plateau (data not shown). The influx rate was approximately four times lower compared to the initial  $\text{TMA}^+$  influx rate detected in normal slices.

### Probe detection by MR spectroscopy

An independent measurement of  $\text{SbF}_6^-$  degradation in a solution of ACSF was made possible by MR spectroscopy. Fig. 5a shows a subset of  $^{19}\text{F}$  magnitude spectra obtained at different time points over a period of 2 hours after the probe solution had been prepared. Based on comparison with the spectrum of a fresh probe solution in NaCl, the broad peak at 5 ppm was assigned to  $\text{SbF}_6^-$ . Interestingly, another fluorine peak, likely a  $\text{SbF}_6^-$  degradation product, had appeared already at 15 min at -30 ppm. It gradually grew and shifted with time, possibly due to changing acidity of the solution.

Absolute concentrations cannot be reliably established with the simple spectroscopic method we employed. However, relative measurements can readily be made and we were able to compare the rates of degradation obtained by ISMs and by MR spectroscopy. This is illustrated



in Fig. 5b where it is demonstrated that the decay rates obtained by both methods are very similar.

## Discussion

Diffusion probes have been serving as the unassuming worker bees of the RTI method for almost 30 years, without receiving much attention. In particular,  $\text{TMA}^+$  has been used extensively in the studies of brain ECS. Other molecules were called upon less often.  $\text{SbF}_6^-$  was listed as a diffusion probe in the early paper describing the RTI method (Nicholson and Phillips, 1981) and played a pivotal role in a spreading depression study (Phillips and Nicholson, 1981; Nicholson and Kraig, 1981). MR diffusion imaging is a much younger method than RTI, and diffusion probes other than water are not very common. A combination of RTI and MR measurements using a single probe could bring new insight and help interpret the complex MR diffusion signal, however, this requires a reliable diffusion probe with well-established characteristics. Our goal was to develop a minimum set of desirable characteristics for such a probe. These were then examined in detail in  $\text{TMA}^+$  and  $\text{SbF}_6^-$ . The main results are summarized in a simplified form in Table I. Clearly, neither probe proved to be an ideal candidate for a combined RTI and MR diffusion study. Several of the enumerated properties impose limitations even on a stand-alone RTI or MR experiment.

Perhaps the most surprising finding is that  $\text{TMA}^+$  penetrates into the cells and accumulates there. The mechanism of this accumulation is unclear,  $\text{TMA}^+$  has generally been regarded as an impermeant cation. If it were passively permeable and its extracellular concentration was small, it should enter cells until its distribution conformed to the Nernst equation, i.e., it should ultimately be about 30 times more concentrated inside the cells than outside. If the cells lost their resting potential then the concentrations should simply equalize. Clearly, the experiments showed that the final distribution of  $\text{TMA}^+$  is not compatible with electrochemical equilibrium of a passively permeable cation because the intracellular concentration ends up too low. Interestingly, Ballanyi et al. (1990) noted a very similar distribution of  $\text{TMA}^+$  and choline (5–15 mM intracellular concentration 0.5–1 hours after 5 mM extracellular application) in the neuropile glial cells of the leech. Ballanyi and Schlue (1989) had earlier postulated that  $\text{TMA}^+$  might enter these glial cells through an acetylcholine-mediated cation channel but the mechanism remained unclear. In particular, some form of active transport cannot be excluded. Another caveat must be made concerning our result, namely that we measured a homogenate of all the cells in the rat brain slice, including both neurons and glia. It is possible that  $\text{TMA}^+$  only enters a subset of these cells but does so at a higher rate and attains a higher level in those cells than we estimated. This issue did not arise with the measurements of Ballanyi and co-workers who used intracellular ISMs to measure  $\text{TMA}^+$  concentration.

Irrespective of the exact mechanism, intracellular accumulation of  $\text{TMA}^+$  has several implications. First, cellular influx happens in such a short time that it precludes MR detection of the exclusively extracellular component of the signal. After the brain tissue becomes exposed to a probe solution, the probe is distributed by diffusion from the tissue surface. This process takes on the order of tens of minutes in a normal brain slice 400  $\mu\text{m}$  thick, and much longer in an ischemic slice or deeper in a brain *in vivo*. By the time  $\text{TMA}^+$  concentrations sufficiently equalize within the ECS, the intracellular concentrations will have grown as well. A typical incubation time of several hours would result in most of the MR signal originating inside the cells. The homogenization experiments in healthy slices suggest that the intracellular compartment would contribute about 88% of the signal, 7.5 times more than the 12% contribution of the extracellular compartment. The intracellular influx and accumulation can explain the difficulties in matching the RTI and MR diffusion data (Kroenke et al., 2003). These authors attributed 17% of the MR signal to  $\text{TMA}^+$  molecules accessing pathways longer than 15.5  $\mu\text{m}$ . This percentage is close to our prediction of 12% for the extracellular signal

component. It is therefore likely that the rest of the signal was intracellular, modulated by the statistical distribution of the cellular dimensions. If a significant number of cells or cellular processes larger than 15.5  $\mu\text{m}$  were present in their sample volume, the extracellular portion of the MR signal would be lower than 17%.

RTI measurements are less affected by the fast cellular uptake of the probe. The ISM detects exclusively the extracellular signal, and a single measurement is completed within minutes. Furthermore, a linear nonspecific clearance term is typically added to the diffusion equation (Nicholson, 1992), approximating any loss of probe that is proportional to its ECS concentration. However, an important question for the RTI method with the  $\text{TMA}^+$  probe remains: The rapid  $\text{TMA}^+$  accumulation inside the cells may be an active process involving energy consumption and redistribution of electric charge. Even though no significant effect of  $\text{TMA}^+$  on the tissue viability has been observed, some interaction of  $\text{TMA}^+$  with the cell physiology is possible. This uncertainty is indicated in Table I.

The most problematic property of the  $\text{SbF}_6^-$  probe is far less subtle: this probe suffers from degradation over time. More importantly, the rate of degradation is not constant or otherwise easily characterized. It was found to depend on temperature, on depth within the brain tissue, and on its ischemic condition. Furthermore, this probe proved detrimental to the health of the brain slices. It is likely that the breakdown of  $\text{SbF}_6^-$  releases fluoride and it is well established that this compound is a very general inhibitor of the glycolytic pathway in cells (Dorfman, 1943). Inhibition of this pathway would eventually shut down the sources of production of energy in a cell and result in ischemia-like conditions leading to cellular swelling. Lower bath concentrations may alleviate this problem but the probe degradation conspires against this solution because it diminishes the remaining available signal.

One advantage of the  $\text{SbF}_6^-$  probe is its slower rate of cellular influx, possibly because the electrochemical equilibrium in cells with a normal resting potential for this anion will favor a low intracellular concentration. Even though the probe degradation made quantitative assessment in terms of absolute intracellular concentrations difficult, the relative increase over time was much slower than in  $\text{TMA}^+$ , and it did not depend as much on tissue ischemia.

Another advantage of  $\text{SbF}_6^-$  is common to all fluorine substances. Because  $^{19}\text{F}$  is not naturally present in biological materials and possesses a large gyromagnetic ratio, its MR detection is relatively simple, without the need for sophisticated spectroscopic techniques or even water signal suppression.  $\text{TMA}^+$  detection, based on its  $^1\text{H}$  signal, is more involved. One may thus inquire if another fluorine substance detectable by both RTI and MR could be found. Hexafluoroarsenate,  $\text{AsF}_6^-$ , a smaller relative of  $\text{SbF}_6^-$ , was previously employed in an RTI study (Nicholson and Phillips, 1981). Unfortunately, our preliminary study indicated that its relaxation time constants are too short for any meaningful MR measurement of brain tortuosity. The probe molecules must be given sufficient time for random walk explorations of this geometrically complex environment, or the tortuosity will be underestimated (Hrabe et al., 2004).

In summary, we believe that a diffusion probe should be carefully tested before it is used by RTI method, MR method, or their combination. We suggest a testing framework based on Table I. The significance of any one characteristic will necessarily depend on details of the intended experiment. However, for the widest possible range of applications, we can presently recommend only the  $\text{TMA}^+$  probe, only for the RTI applications, and only when its intracellular accumulation can be tolerated.

## Acknowledgments

This work was supported primarily by NIH grant NS045797 (to JH), and in part by NIH grants NS47557 (to SH) and NS28642 (to CN).

## References

- Ammann D, Chao P, Simon W. Valinomycin-based  $K^+$  selective microelectrodes with low electrical resistance. *Neurosci. Lett* 1987;74:221–226. [PubMed: 3574760]
- Ballanyi K, Grafe P, Serve G, Schlue WR. Electrophysiological measurements of volume changes in leech neuropile glial cells. *Glia* 1990;3:151–158. [PubMed: 2141591]
- Ballanyi K, Schlue WR. Electrophysiological characterization of a nicotinic acetylcholine receptor on leech neuropile glial cells. *Glia* 1989;2:330–345. [PubMed: 2530172]
- Basser PJ, Mattiello J, LeBihan D. MR diffusion tensor spectroscopy and imaging. *Biophys. J* 1994;66:259–267. [PubMed: 8130344]
- Dorfman A. Pathways of glycolysis. *Physiol. Rev* 1943;23:124–138.
- Hrabe J, Hrabetova S, Segeth K. A model of effective diffusion and tortuosity in the extracellular space of the brain. *Biophys. J* 2004;87:1606–1617. [PubMed: 15345540]
- Hrabetova S, Nicholson C. Dextran decreases extracellular tortuosity in thick-slice ischemia model. *J. Cereb. Blood Flow Metab* 2000;20:1306–1310. [PubMed: 10994852]
- Hrabetova, S.; Nicholson, C. Biophysical properties of brain extracellular space explored with ion-selective microelectrodes, integrative optical imaging and related techniques. In: Michael, AC.; Borland, LM., editors. *Electrochemical Methods for Neuroscience*. Boca Raton: CRC Press; 2007. p. 167-204.
- Hrabetova S, Chen KC, Masri D, Nicholson C. Water compartmentalization and spread of ischemic injury in thick-slice ischemia model. *J. Cereb. Blood Flow Metab* 2002;22:80–88. [PubMed: 11807397]
- Hrabetova S, Hrabe J, Nicholson C. Dead-space microdomains hinder extracellular diffusion in rat neocortex during ischemia. *J. Neurosci* 2003;23:8351–8359. [PubMed: 12967997]
- Krizaj D, Rice ME, Wardle RA, Nicholson C. Water compartmentalization and extracellular tortuosity after osmotic changes in cerebellum of *Trachemys Scripta*. *J. Physiol* 1996;492:887–896. [PubMed: 8734998]
- Kroenke CD, Ackerman JJH, Neil JJ. Magnetic resonance measurement of tetramethylammonium diffusion in rat brain: comparison of magnetic resonance and ionophoresis in vivo diffusion measurements. *Magn. Reson. Med* 2003;50:717–726. [PubMed: 14523957]
- Kume-Kick J, Mazel T, Vorisek I, Hrabetova S, Tao L, Nicholson C. Independence of extracellular tortuosity and volume fraction during osmotic challenge in rat neocortex. *J. Physiol* 2002;542:515–527. [PubMed: 12122149]
- Lehmenkühler A, Sykova E, Svoboda J, Zilles K, Nicholson C. Extracellular space parameters in the rat neocortex and subcortical white matter during postnatal development determined by diffusion analysis. *Neuroscience* 1993;55:339–351. [PubMed: 8377929]
- Mazel T, Richter F, Vargova L, Sykova E. Changes in extracellular space volume and geometry induced by cortical spreading depression in immature and adult rats. *Physiol. Res* 2002;51:85–93. [PubMed: 12071295]
- Nicholson C, Hounsgaard J. Diffusion in the slice microenvironment and implications for physiological studies. *Federation Proc* 1983;42:2865–2868. [PubMed: 6350048]
- Nicholson, C.; Kraig, RP. The behaviour of extracellular ions during spreading depression. In: Zeuthen, T., editor. *The application of ion-selective electrodes*. Amsterdam: Elsevier; 1981. p. 217-238.
- Nicholson C, Phillips JM. Ion diffusion modified by tortuosity and volume fraction in the extracellular microenvironment of the rat cerebellum. *J. Physiol* 1981;321:225–257. [PubMed: 7338810]
- Nicholson C. Quantitative analysis of extracellular space using the method of  $TMA^+$  iontophoresis and the issue of  $TMA^+$  uptake. *Can. J. Physiol. Pharmacol* 1992;70:314–322.
- Nicholson C. Ion-selective microelectrodes and diffusion measurements as tools to explore the brain cell microenvironment. *J. Neurosci. Methods* 1993;48:199–213. [PubMed: 8412303]

- Nicholson C. Diffusion and related transport mechanisms in brain tissue. *Rep. Prog. Phys* 2001;64:815–884.
- Phillips, JM.; Nicholson, C. Microelectrodes for novel anions and their application to some neurophysiological problems. In: Lübbers, DW.; Acker, H.; Buck, RP.; Eisenman, G.; Kessler, M.; Simon, W., editors. *Progress in enzyme and ion-selective electrodes*. Berlin: Springer-Verlag; 1981. p. 15-20.
- Quirk JD, Bretthorst GL, Duong TQ, Snyder AZ, Springer CS Jr, Ackerman JJ, Neil JJ. Equilibrium water exchange between the intra- and extracellular spaces of mammalian brain. *Magn. Reson. Med* 2003;50:493–499. [PubMed: 12939756]
- Rice ME, Nicholson C. Diffusion characteristics and extracellular volume fraction during normoxia and hypoxia in slices of rat neostriatum. *J. Neurophysiol* 1991;65:264–272. [PubMed: 2016641]
- Schwindt W, Nicholson C, Lehmenkühler A. Critical volume of rat cortex and extracellular threshold concentration for a pentylenetetrazol-induced epileptic focus. *Brain Res* 1997;753:86–97. [PubMed: 9125435]
- Slais K, Vorisek I, Zoremba N, Homola A, Dmytrenko L, Sykova E. Brain metabolism and diffusion in the rat cerebral cortex during pilocarpine-induced status epilepticus. *Exp. Neurol* 2008;209:145–154. [PubMed: 17961555]
- Somjen GG. Mechanisms of spreading depression and hypoxic spreading depression-like depolarization. *Physiol. Rev* 2001;81:1065–1096. [PubMed: 11427692]
- Sykova E, Svoboda J, Polak J, Chvatal A. Extracellular volume fraction and diffusion characteristics during progressive ischemia and terminal anoxia in the spinal cord of the rat. *J. Cereb. Blood Flow Metab* 1994;14:301–311. [PubMed: 8113325]
- Sykova E, Mazel T, Simonova Z. Diffusion constraints and neuron-glia interaction during aging. *Exp. Gerontol* 1998;33:837–851. [PubMed: 9951627]
- Sykova E, Mazel T, Hasenohrl RU, Harvey AR, Simonova Z, Mulders WH, Huston JP. Learning deficits in aged rats related to decrease in extracellular volume and loss of diffusion anisotropy in hippocampus. *Hippocampus* 2002;12:269–279. [PubMed: 12000123]
- Vorisek I, Sykova E. Evolution of anisotropic diffusion in the developing rat corpus callosum. *J. Neurophysiol* 1997;78:912–919. [PubMed: 9307124]
- Wick M, Nagatomo Y, Prielmeier F, Frahm J. Alteration of intracellular metabolite diffusion in rat brain in vivo during ischemia and reperfusion. *Stroke* 1995;26:1930–1933. [PubMed: 7570750]

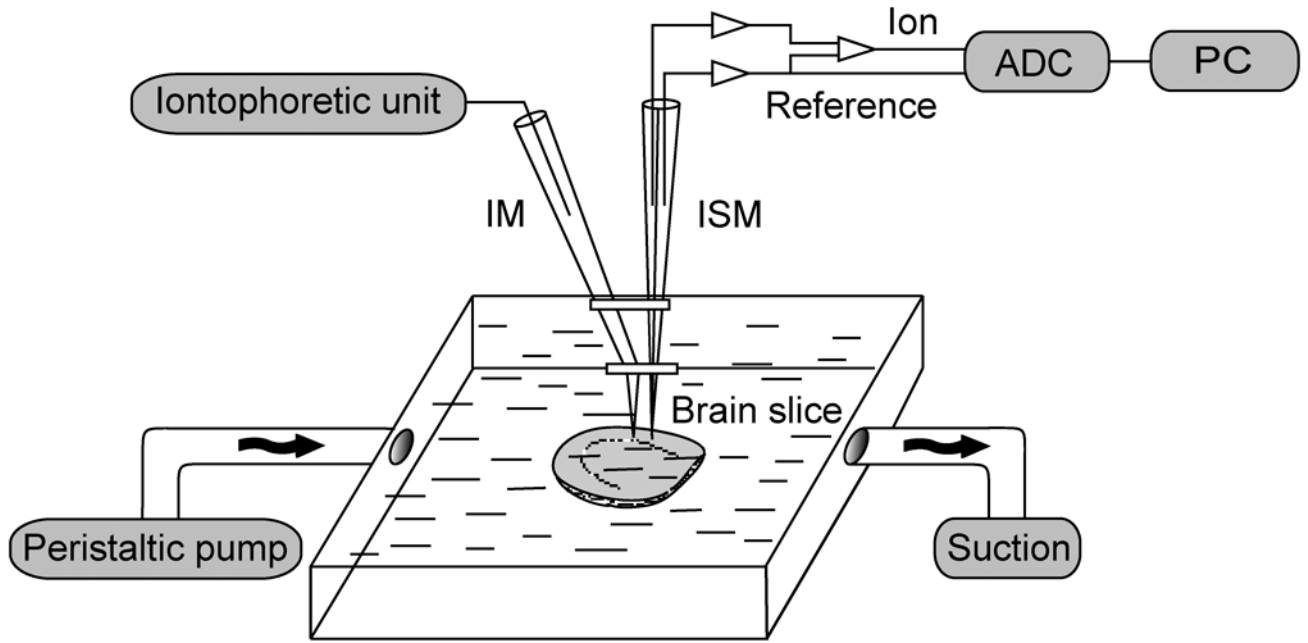


**Figure 1.**

Schematic drawing of a setup used for probe stability measurements in the brain tissue as well as for RTI measurements. The iontophoretic unit and the corresponding iontophoretic microelectrode (IM) were only necessary for the RTI measurements. Inflow of ACSF into the chamber was supplied by a peristaltic pump, and the bath level was maintained 1–2 mm above the slice by vertical positioning of a vacuum suction outlet. The ion-selective microelectrode (ISM) signal was digitized by analog to digital converter (ADC) and stored on a personal computer (PC). Diffusion measurements in agar were obtained in a separate well placed inside the chamber (not shown).

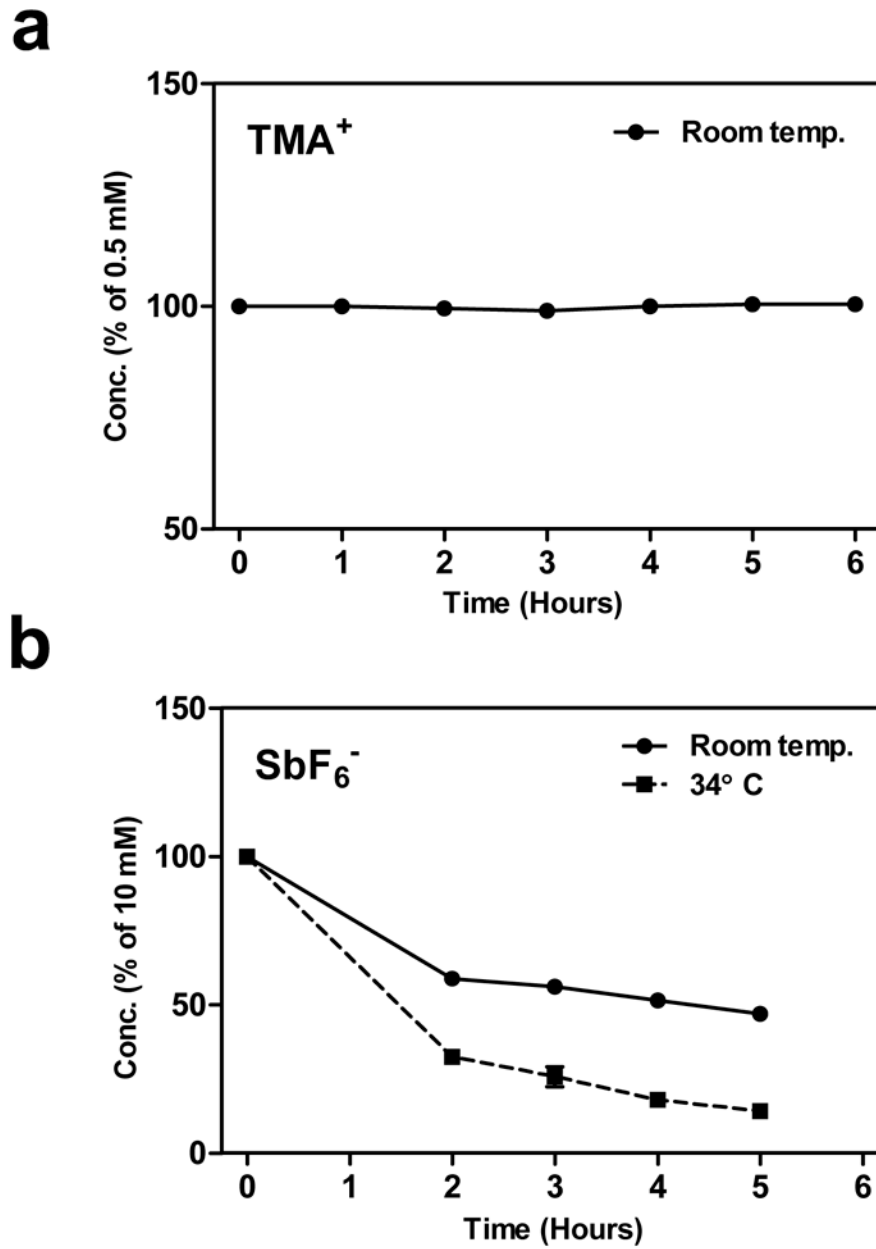


**Figure 2.**

**a)** Stability of TMA<sup>+</sup> probe. Solution of the probe (0.5 mM) in ACSF was repeatedly tested by ISM. Every data point represents an average of 4–8 measurements, vertical bars indicate SEMs but they are smaller than the point symbols. **b)** The same experiment with the SbF<sub>6</sub><sup>-</sup> probe (10 mM solution) at room temperature and at 34°C.



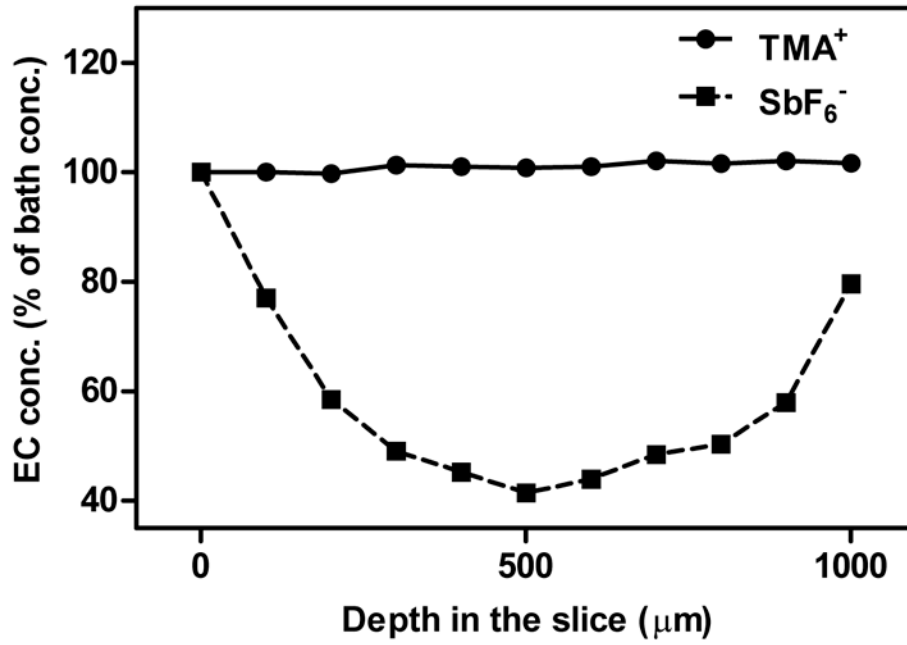


**Figure 3.** Probe concentration profiles obtained across ischemic (1000  $\mu\text{m}$ ) brain slices at room temperature. Incubation periods in  $\text{SbF}_6^-$  (5 mM bath) or  $\text{TMA}^+$  (4 mM bath) lasted at least 1 hour. Bath concentrations represent 100% on the vertical axis of the graph,  $n = 3$ .

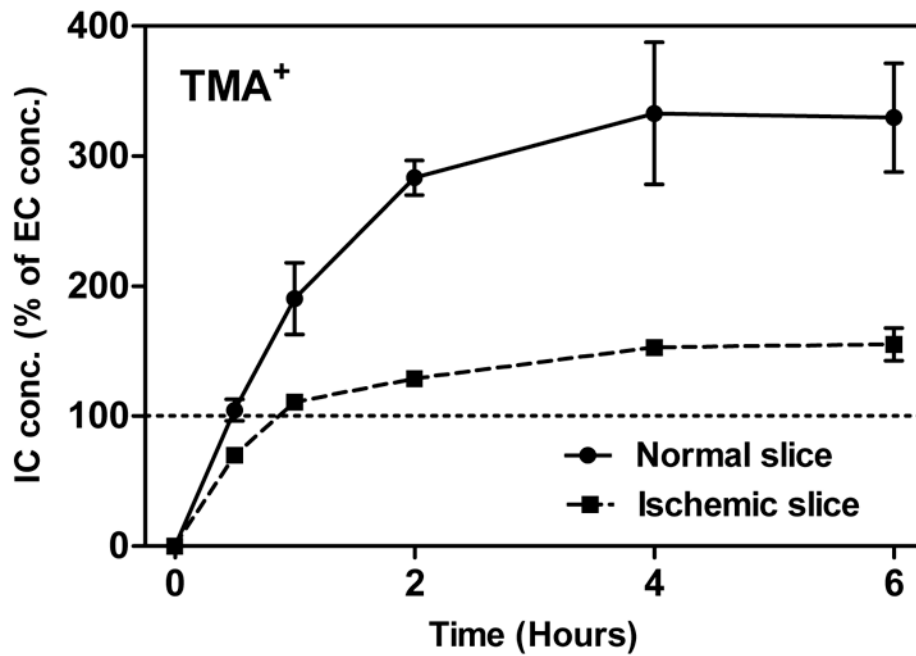


**Figure 4.** Intracellular concentration of TMA<sup>+</sup> as a function of incubation time at room temperature. The bath concentration of TMA<sup>+</sup> was 0.5 mM, represented by 100% in the graph. Intracellular concentrations were calculated from Eq. (5). At least 3 measurements were obtained at every time point for ischemic slices, and at least 5 for normal slices. Data points are the mean values, vertical bars show SEM. The value at time zero is theoretical.

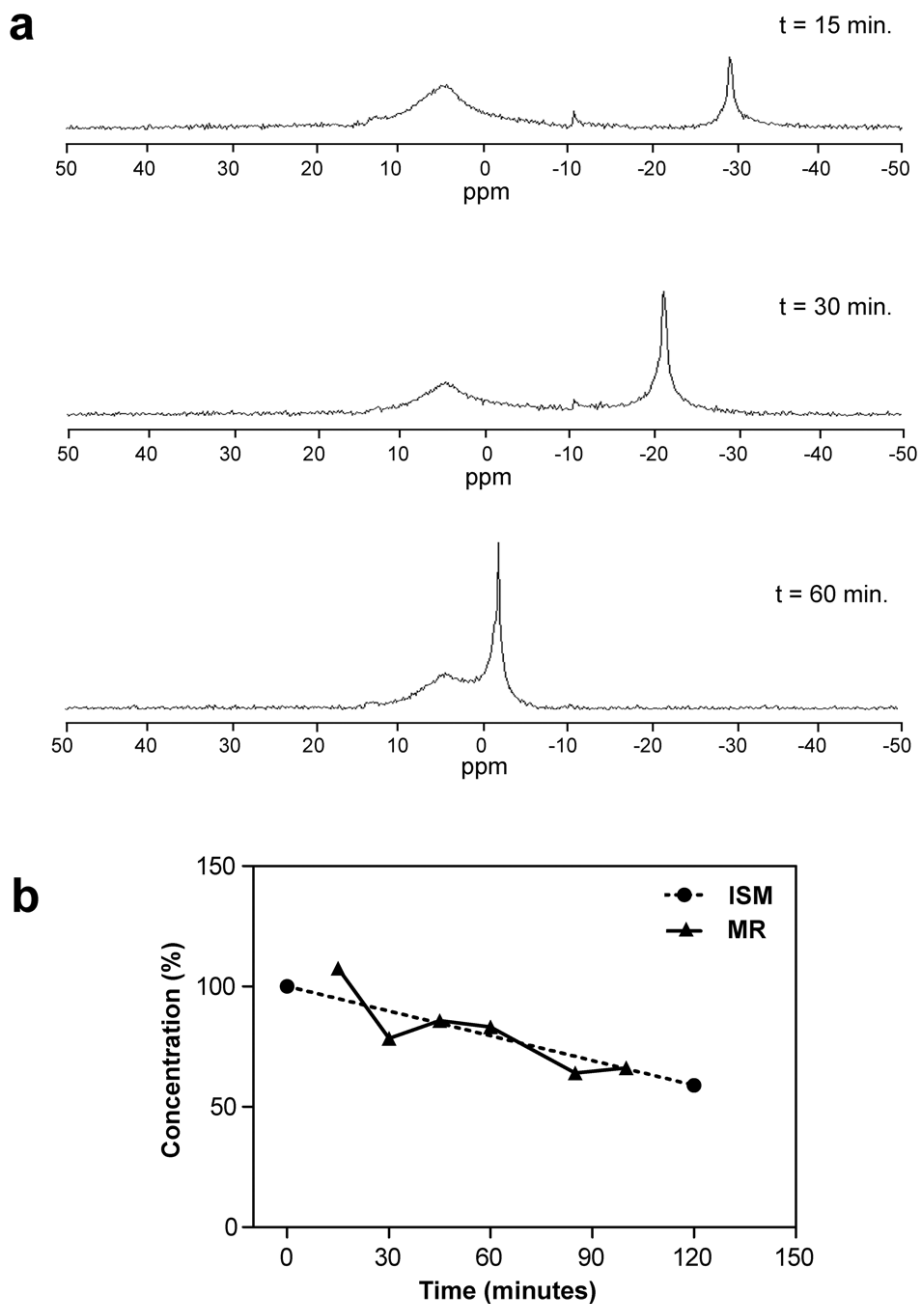


**Figure 5.**  
**a)** The  $^{19}\text{F}$  MR spectra obtained from 10 mM solution of  $\text{SbF}_6^-$  in ACSF at room temperature. Six spectra were collected over 100 min. but only 3 representative results are shown. The horizontal axis is calibrated in parts per million (ppm) and follows the spectroscopic convention of growing more positive leftward. The broader peak represents the probe, the narrower peak is likely formed by a product of its degradation, possibly HF. **b)** A comparison of relative degradation rates obtained by ISM (data from Fig. 2b) and by MR spectroscopy (data from Fig. 5a). Only relative changes in concentration were obtained by the MR method, and both data sets were therefore normalized to the same mean value to make the comparison of rates easier.

**Table I**Desirable characteristics of diffusion probes and their evaluation in TMA<sup>+</sup> and SbF<sub>6</sub><sup>-</sup>

Characteristic	TMA <sup>+</sup>	SbF <sub>6</sub> <sup>-</sup>
Predictable diffusion properties	Yes	Yes
Chemical stability	Yes	No
Negligible effect on neurophysiology	Qualified yes	No
Slow rate of cellular penetration	No	Qualified yes
Detectability by ISMs	Yes	Yes
Detectability by MR	Yes	Yes